MHD Boundary Layer Heat and Mass Transfer Flow Ofnanofluid Through Porous Media Over an Inclined Plate with Chemical Reaction

V.RamachandraReddy[a, *], M. SuryanarayanaReddy[b]
[a]Research Scholar, Department of Mathematics, JNTUA, Anathapuramu, A.P, India.
Assistant Professor, Department of Mathematics, JNTUACE, Pulivendula, A.P. India.

Abstract

Steady- state mixed convection boundary layer flow, heat and mass transfer characteristics of Kuznetsov and Nield model nanofluid over an inclined porous vertical plate with thermal radiation and chemical reaction is presented in this analysis. The governing non-linear partial differential equations represents the flow model can be converted into system of non-linear ordinary differential equations using the similarity variables and are solved numerically using finite element method. The effect of various pertinent parameters on velocity, temperature and concentration distributions is calculated.The rates of non-dimensional temperature and concentration are both decelerate with the rising values of (*Nt*).

Keywords: Heat and Mass transfer; Inclined plate; Nanofluid; Chemical reaction; Finite element method.

1. Introduction

In recent years the concept of nanofluids has become most prominent area because of its extensive range of applications. Keeping this in mind several authors [1, 2, 3, 4] has done good work on heat transfer enhancement of various nanofluids.Oztopet al. [5] have discussed heat and mass transfer characteristics of Al_2O_3 - water, TiO_2 - water and CuO - water nanofluids over two-dimensional rectangular enclosures.Aminossadatiet al. [6]discussed the heat transfer analysis of Cu, Ag, Al_2O_3 and TiO_2 nanoparticles.FakhreddineSegni et al. [7] perceived heat trasfer enhancement of Al_2O_3, TiO_2 and Cu nanoparticles overa two-dimensional cavity. Sudarsana Reddy et al. [8] have noted natural convection heat transfer deterioration in the both $Al_2O_3 - water$ and $Ag - water$ based nanofluids over a vertical cone.Teamah et al. [9] have analyzed the impact of magnetic field and heat source on natural convection flow over rectangular enclosure. Chamkha et al. [10] have studied free convection flow of nanofluid over a vertical plate with the influence of magnetic field and heat generation/absorption. Ranaet al. [11] reported mixed convection boundary layer flow, heat and mass transfer over a vertical plate through porous medium filled with nanofluid with heat generation/absorption. Gorla et al. [12] discussed boundary layer natural convection over a horizontal plate embedded in a nanofluid saturated porous medium. Khan et al. [13] have analyzed natural convection boundary layer flow over a vertical plate by taking uniform surface heat flux boundary condition. Aziz et al. [14] noticed boundary layer flow of a nanofluid over a convectively heated vertical plate. Uddin et al. [15] have reported MHD boundary layer flow, heat and mass transfer characteristics past a flat vertical plate.Kuznetsov and Nield [16] have extended the Cheng–Minkowycz problem for boundary layer flowover a vertical plate embedded in nanofluid saturated porous medium. Noghrehabadiet al. [17] have analyzed the natural convection boundary layer flow over a nanofluid saturated porous vertical plate with prescribed surface heat flux. Olanrewaju et al. [18] have presented the boundary layer stagnation point flow over a permeable plat surface through porous medium filled with nanofluid.Ibrahim et al. [19], Ghalambaz et al. [20], have also discussed the natural convection boundary layer heat and mass transfer analysis of nanofluid through porous medium over vertical plate. Chamkha et al. [21] presented the boundary layer features of nanofluidsthrough porous media.Gorlaet al. [22] have analyzed the natural convection of nanofluid over a vertical cone embedded in porous medium. Das et al. [23] presented the influence of radiation on nanofluid flow over unsteady stretching surface.Zaraki et al. [24] presented heat and mass transfer characteristics of nanofluids.

2. Mathematical Analysis

We consider natural convention boundary layer flow, heat and mass transfer over an inclined plate embedded in a nanofluid-saturated porous medium, with an acute angle α to the vertical, as illustrated in Fig.1. T_w and ϕ_w are uniform temperature and concentration at surface and are assumed to be greater than the ambient temperature and concentration T_∞ andϕ_∞ respectively. A constant magnetic field of strength B_0 is applied in the direction of the *y*-axis.

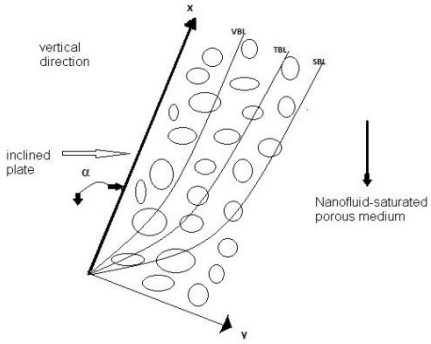

Fig. 1.Flow configuration and coordinate system.

$$\frac{\partial u}{\partial x}+\frac{\partial v}{\partial y}=0 \quad (1)$$

$$\rho\left(u\frac{\partial u}{\partial x}+v\frac{\partial u}{\partial y}\right)=\mu\frac{\partial^2 u}{\partial y^2}-\frac{\mu}{k}u+$$
$$g\left[(1-\phi_\infty)\rho_{f\infty}\beta(T-T_\infty)-(\rho_p-\rho_{f\infty})(\phi-\phi_\infty)\right]Cos\gamma-\sigma B_0{}^2u \quad (2)$$

$$u\frac{\partial T}{\partial x}+v\frac{\partial T}{\partial y}=\alpha\frac{\partial^2 T}{\partial y^2}+\tau\left[D_B\frac{\partial\phi}{\partial y}.\frac{\partial T}{\partial y}+\left(\frac{D_T}{T_\infty}\right)\left(\frac{\partial T}{\partial y}\right)^2\right]-\frac{1}{\rho c_p}\frac{\partial q_r}{\partial y} \quad (3)$$

$$u\frac{\partial\phi}{\partial x}+v\frac{\partial\phi}{\partial y}=D_B\frac{\partial^2\phi}{\partial y^2}+\left(\frac{D_T}{T_\infty}\right)\frac{\partial^2 T}{\partial y^2}-K_r(\phi-\phi_\infty) \quad (4)$$

The associated boundary conditions are

$$u=0,\ v=0,\ T=T_w,\quad \phi=\phi_w\, at\, y=0 \quad (5)$$
$$u\to 0,\quad T\longrightarrow T_\infty,\quad \phi\longrightarrow\phi_\infty\, at\, y\to\infty \quad (6)$$

The radiative heat flux q_r(using Rosseland approximation) is defined as

$$q_r=-\frac{4\sigma^*}{3K^*}\frac{\partial T^4}{\partial y}, \quad (7)$$

By using Taylor series expansion and after neglecting higher-order terms, we get

$$T^4\cong 4T_\infty{}^3T-3T_\infty{}^4\,. \quad (8)$$

Thus substituting Eq. (8) in Eq. (7), we get

$$q_r=-\frac{16T_\infty{}^3\sigma^*}{3K^*}\frac{\partial T}{\partial y}. \quad (9)$$

The similarity variables are defined as

$$\eta=\frac{y}{x}Ra_x^{1/4},\ s(\eta)=\frac{\psi}{\alpha\, Ra_x^{1/4}},\quad \theta(\eta)=\frac{T-T_\infty}{T_w-T_\infty},\quad f(\eta)=\frac{\phi-\phi_\infty}{\phi_w-\phi_\infty} \quad (10)$$

where, $Ra_x=\frac{g\beta\rho_{f\infty}(T_w-T_\infty)(1-\phi_\infty)x^3}{\mu\,\alpha}$, is the Rayleigh number.

Substituting Eqns. (9) *and* (10) into Eqns. (1) – (4), we obtain the following non-linear ordinary differential equations

$$s'''+\frac{1}{Pr}\left(\frac{3}{4}ss''-\frac{1}{2}(s')^2\right)+(\theta-Nr\,f)\,Cos\,\gamma-(M+K)s'=0 \quad (11)$$
$$(1+R)\theta''+\frac{3}{4}\,s\theta'+Nb\,\theta'f'+Nt(\theta')^2=0 \quad (12)$$
$$f''+\frac{3}{4}Le\,s\,f'-Cr.f+\frac{Nt}{Nb}\theta''=0 \quad (13)$$

The transformed boundary conditions are

$$\eta=0,\quad s=0,\quad s'=1,\quad \theta=1,\ f=1.$$
$$\eta\longrightarrow\infty,\quad s'=0,\quad \theta=0,\quad f=0. \quad (14)$$

where,

$$Nr=\frac{(\rho_p-\rho_{f\infty})(\phi_w-\phi_\infty)}{\rho_{f\infty}\beta(T_w-T_\infty)(1-\phi_\infty)},\quad Nb=\frac{\tau D_B(\phi_w-\phi_\infty)}{\alpha},\quad Nt=\frac{\tau D_T(T_w-T_\infty)}{\alpha\,T_\infty},K=\frac{x^2}{k\,Ra_x^{1/2}},$$
$$Le=\frac{\alpha}{D_B},\ Cr=\frac{K_r x^2}{Ra_x^{1/2}},\ Pr=\frac{\mu}{\rho\,\alpha},\ R=\frac{16T_\infty{}^3\sigma^*}{3K^*\alpha\,\rho c_p},\ M=\frac{\sigma\beta_o^2}{\mu\,Ra_x^{1/2}}. \quad (15)$$

The skin-friction coefficient, Nusselt number, and local Sherwood number are defined as

$$C_f=\frac{2\,\tau_w}{\rho},\ Nu=\frac{xq_w}{k(T_w-T_\infty)},\quad Sh=\frac{xJ_w}{D_B(\phi_w-\phi_\infty)} \quad (16)$$

The set of equations (11)– (13)are solved using Finite – elementmethod [25, 26].

3. Results and Discussion

The distributions of velocity, temperature and concentration are presented in Figs. 2 –20. The Comparison ofpresent results with the results reported by PuneetRana*et al.* [27] is made and found good agreement which is shown in Table 1.

The velocity profiles diminish throughout the boundary layer regime with the improving values of magnetic parameter (Fig.2). This additional force raises the thickness of thermal boundary layer, so that the temperature profiles enhance in the flow regime with the rise in *M* (Fig. 3). It is observed from Fig. 4 that the velocity profiles decelerate as the values of (*Nr*) increases. The temperature profiles of the fluid increases with increasing values of buoyancy ratio parameter (Fig 5).

The hydrodynamic boundary layer thickness deteriorates with improving values of plate inclination angle (γ) as shown inFig.6. It is perceivedthat an increase in plate inclination angle (γ) resist the motion of the fluid, which causes an enhancement in the thickness of the thermal boundary layer (Fig 7). The solutal boundary layer thickness is improved in the fluid region with an increase in the values of γ (Fig. 8). Temperature profiles retards with the increasing values of Prandtl number (Fig.9).It is noticed form Fig. 10 that, the thermal boundary layer thickness is enhanced with the higher values of (*R*) in the entire flow region. It is noticed that, the thermal boundary layer thickness improves (Fig.11), whereas solutal boundary layer thickness deteriorates (Fig.12) in the fluid regime with the growing values of Brownian motion parameter (*Nb*).It is perceived from Figs. 13 and 14 that both temperature and concentration profiles elevates in the boundary layer region with the higher values of thermophoretic parameter (*Nt*). It is observed from Fig. 15 that thermal boundary layer thickness deteriorates with the increasing values of the Lewis number in the entire fluid region. We see from figure 16 that the concentration profiles impede with the improving values of chemical reaction parameter (*Cr*).

The values of skin-friction coefficient, Nusselt number and Sherwood number are calculated and are shown in Table 2. It is evident that skin friction coefficient enhances, whereas the Nusselt number and Sherwood number decelerates with the increasing values of (*M*). It is also seen that the skin friction coefficient and Nusselt number decreases whereas Sherwood number elevates with the higher values of (*R*). With the higher values of (*Nb*) the rate of change of velocity and heat transfer rates decelerates whereas mass transfer rates enhances in the boundary layer regime. We have noticed depreciation in the skin friction coefficient with the improving values of (*Nt*). However, Nusselt number and Sherwood number are both increases with an increment in the values of (*Nt*). It is observed from this table that both skin friction coefficient and Nusselt number diminishes while Sherwood number enhances with the improving values of (*Cr*).

4. Conclusion

The values ofskin-friction coefficient $-f''(0)$, Nusselt number $-\theta'(0)$ and Sherwood number $-\phi'(0)$are studied and the results are shown in graphically and in tabular form. The velocity distributions reduced with the rising values of *M*.Nusselt number values diminishesas (*Nr*) improved.

References

[1] S.U.S. Choi, ASME, FED 231/MD, 66, 99 (1995).
[2] J. A. Eastman, S.U.S. Choi, S. Li, W. Yu, L.J. Thompson, Appl. Phys. Lett.78, 718 (2001).
[3] J. Buongiorno, ASME J Heat Transfer, 128, 240 (2006).
[4] K. Khanafer, K. Vafai, M. Lightstone, Int. J Heat Mass Transfer, 46, 3639 (2003).
[5] H. F. Oztop, E. Abu-Nada, Int. J Heat Fluid Flow, 29, 1326 (2008).
[6] S. M. Aminossadati, B. Ghasemi, European J Mechanics-B/Fluids, 28, 630 (2009).
[7] O. FakhreddineSegni, B. Rachid, Nanoscale Research Letters, 6, 222 (2011).
[8] P. Sudarsana Reddy, K. V. SuryanarayanaRao, Procedia Engineering, 127, 476 (2015).
[9] M. A. Teamah, Ahmad F. Elsafty, Enass Z. Massoud, International Journal of Thermal Sciences, 52, 161 (2012).
[10] A. J. Chamkha, A. M. Aly, Chemical Engineering Communications, 198, 425 (2010).
[11] P. Rana, R. Bhargava, Commun. Nonlinear Sci. Numer.Simul.16, 4318 (2011).
[12] R. S. R. Gorla, A. J. Chamkha, J. Mod. Phys. 2, 62 (2011).
[13] W. A. Khan, A. Aziz, International Journal of Thermal Sciences, 50, 1207 (2011).
[14] A. Aziz, W.A. Khan, Int. J. Therm. Sci. 52, 83 (2012).
[15] M. J. Uddin, W. A. Khan, A. I. Ismail, PLoS ONE, 7, e49499 (2012).
[16] A. V. Kuznetsov, D. A. Nield, Int. J. Heat Mass Transfer 65, 682 (2013).
[17] A. Noghrehabadi, A. Behseresht, M. Ghalambaz, Appl. Math. Mech.(English Edition) 34, 669 (2013).
[18] A. M. Olanrewaju, O.D. Makinde, ChemEng Commun.200, 836 (2013).
[19] W. Ibrahim, O. D. Makinde, Comput Fluids 86, 433 (2013).
[20] M. Ghalambaz, A. Noghrehabadi, A. Ghanbarzadeh, Brazilian Journal of Chemical Engineering 31, 413 (2014).
[21] A. J. Chamkha, S. Abbasbandy, A. M. Rashad, International Journal of Numerical Methods for Heat and Fluid Flow 25, 422 (2015).
[22] R. S. R. Gorla, A. J. Chamkha, K. Ghodeswar, J. Nanofluids 3, 65 (2014).
[23] Kalidas Das, P. R. Duari, P. K. Kundu, Alexandria Engineering Journal 53, 737 (2014).
[24] A. Zaraki, M. Ghalambaz, A. J. Chamkha, M. Ghalambaz, D. De Rossi, Advanced Powder Technology 26, 935 (2015).
[25] P. Sudarsana Reddy, A. J. Chamkha, Journal of Naval Architechure and Marine Engineering, 13, 39 (2016).
[26] O. Anwar Bég, H. S. Takhar, R. Bhargava, S. Rawat, V. R. Prasad, Phys. Scr. 77, 1 (2008).
[27] P. Rana, R. Bhargava, O.A. Beg, Computers and Mathematics with Applications 64, 2816 (2012).

Table 1. Comparison of present results with previously published work, for Nr=0.5, $\gamma = \frac{\pi}{6}$, M=0, R = 0, Cr = 0.

Parameter			$-\theta'(0)$		$-\phi'(0)$	
Le	Nt	Nb	P. Rana et al. [27]	Present Results	P.Rana et al. [27]	Present Results
5.0	0.1	0.5	0.4425	0.4430	1.5101	1.5104
5.0	0.1	1.0	0.3025	0.3029	1.5433	1.5436
5.0	0.1	1.5	0.0879	0.0875	1.5693	1.5687
5.0	0.3	0.5	0.4064	0.4068	1.5106	1.5112
5.0	0.3	1.0	0.2779	0.2785	1.5601	1.5606
5.0	0.3	1.5	0.0807	0.0801	1.5855	1.5849
5.0	0.5	0.5	0.3742	0.3747	1.5194	1.5198
5.0	0.5	1.0	0.2559	0.2563	1.5803	1.5812
5.0	0.5	1.5	0.0742	0.0735	1.6013	1.6006

Table 2. The values of skin-friction coefficient, Nusselt number and Sherwood number.

M	R	Nb	Nt	Cr	$-f''(0)$	$-\theta'(0)$	$-\phi'(0)$
0.1	0.1	0.5	0.5	0.1	0.89497	0.29893	0.61814
0.2	0.1	0.5	0.5	0.1	0.94344	0.29407	0.61210
0.3	0.1	0.5	0.5	0.1	0.99014	0.28943	0.60643
0.4	0.1	0.5	0.5	0.1	1.03525	0.28499	0.60111
0.5	0.1	0.5	0.5	0.1	1.07888	0.28074	0.59612
0.1	0.01	0.5	0.5	0.1	1.08346	0.28710	0.59020
0.1	0.15	0.5	0.5	0.1	1.07650	0.27734	0.59925
0.1	0.3	0.5	0.5	0.1	1.06998	0.26766	0.60804
0.1	0.45	0.5	0.5	0.1	1.06430	0.25879	0.61595
0.1	0.6	0.5	0.5	0.1	1.06248	0.25601	0.61841
0.1	0.1	0.2	0.5	0.1	1.07489	0.32338	0.68081
0.1	0.1	0.5	0.5	0.1	1.07720	0.30108	0.63324
0.1	0.1	0.7	0.5	0.1	1.07888	0.28074	0.59612
0.1	0.1	1.2	0.5	0.1	1.07997	0.26220	0.56784
0.1	0.1	1.5	0.5	0.1	1.08054	0.24529	0.56470
0.1	0.1	0.5	0.1	0.1	1.10510	0.34909	0.44400
0.1	0.1	0.5	0.3	0.1	1.07720	0.30108	0.63324
0.1	0.1	0.5	0.5	0.1	1.06438	0.25344	0.68023
0.1	0.1	0.5	0.7	0.1	1.05472	0.21143	0.70114
0.1	0.1	0.5	1.0	0.1	1.04403	0.16436	0.71554
0.1	0.1	0.5	0.5	0.1	1.07843	0.28057	0.59913
0.1	0.1	0.5	0.5	0.2	1.07185	0.27788	0.69985
0.1	0.1	0.5	0.5	0.3	1.06666	0.27574	0.78592
0.1	0.1	0.5	0.5	0.4	1.06240	0.27397	0.86190
0.1	0.1	0.5	0.5	0.5	1.05880	0.27247	0.93047

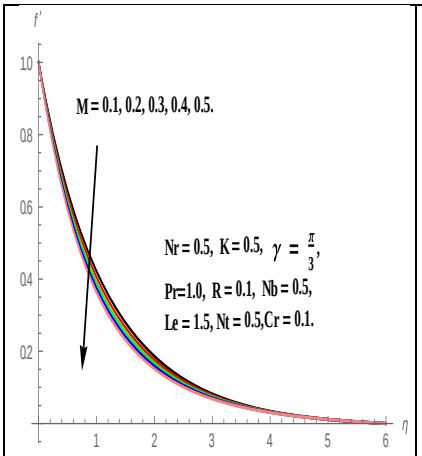

Fig.2. Effect of Mon f'.

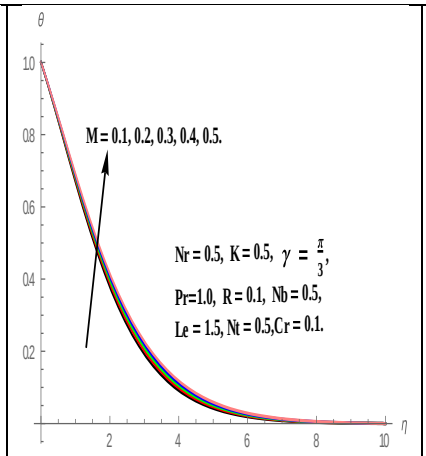

Fig. 3. Effect of M on θ.

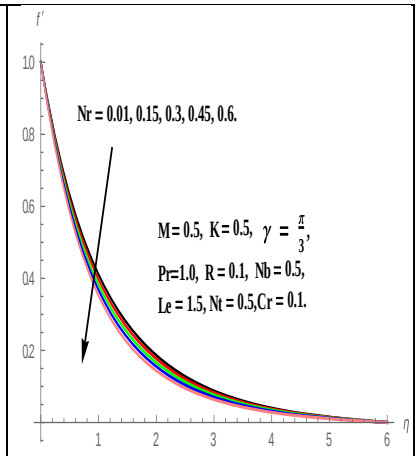

Fig. 4. Effect of Nron f'.

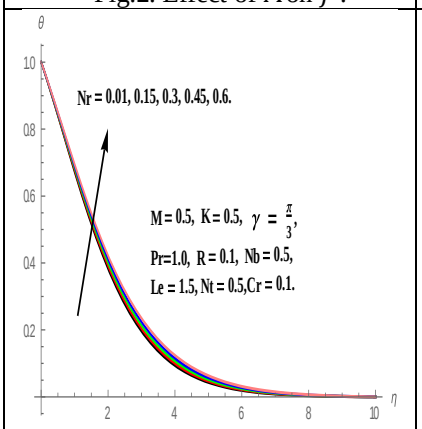

Fig. 5. Effect of Nr on θ.

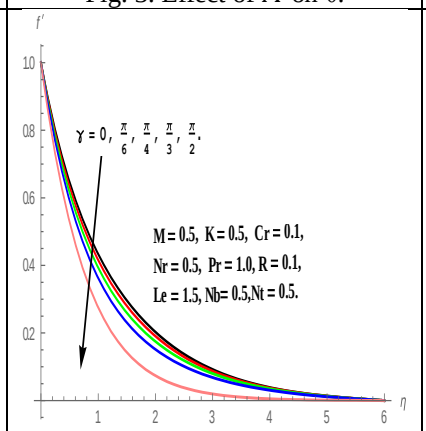

Fig. 6. Effect of γon f'.

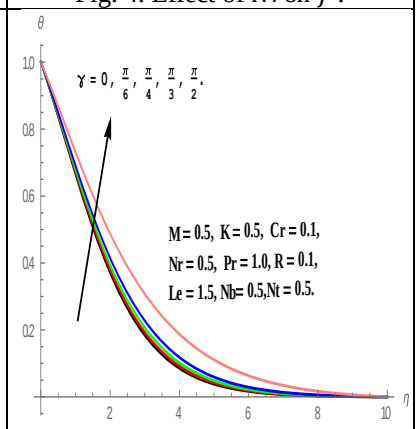

Fig. 7. Effect of γ on θ.

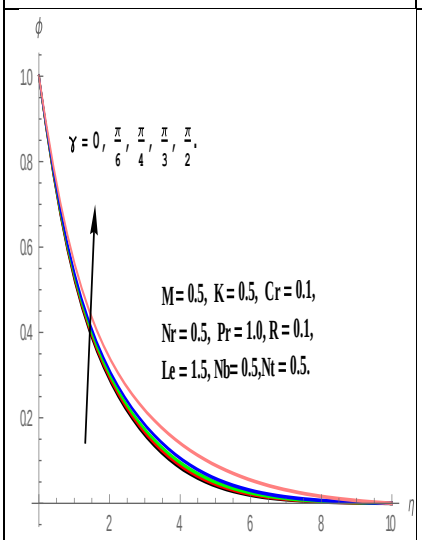

Fig. 8. Effect of γ on ϕ.

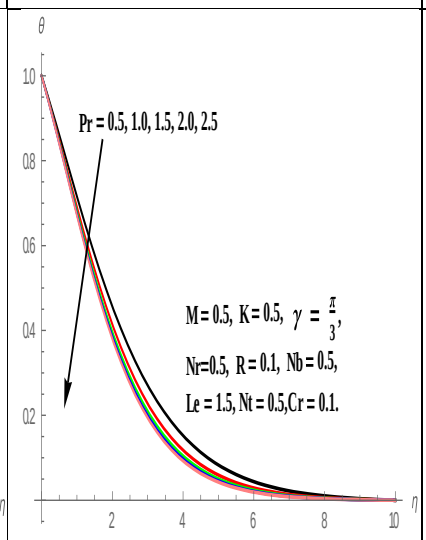

Fig. 9. Effect of Pr on θ.

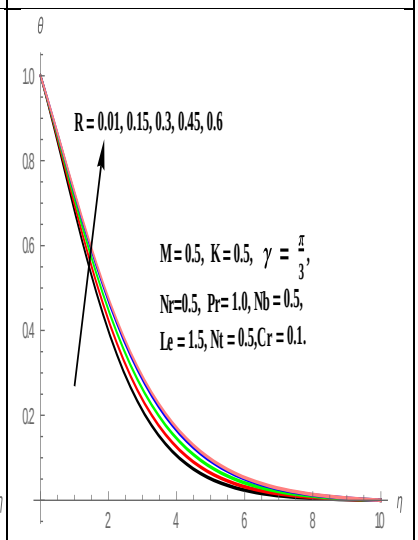

Fig. 10. Effect of R on θ.

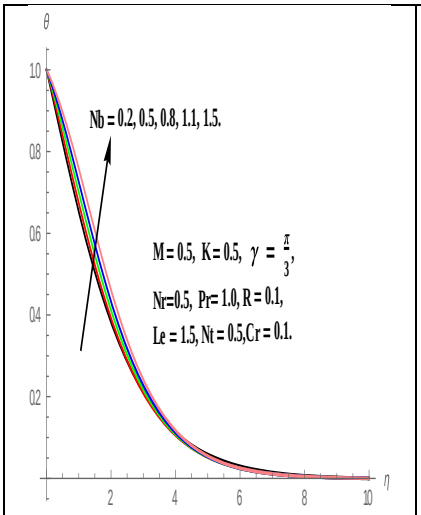

Fig. 11. Effect of Nb on θ.

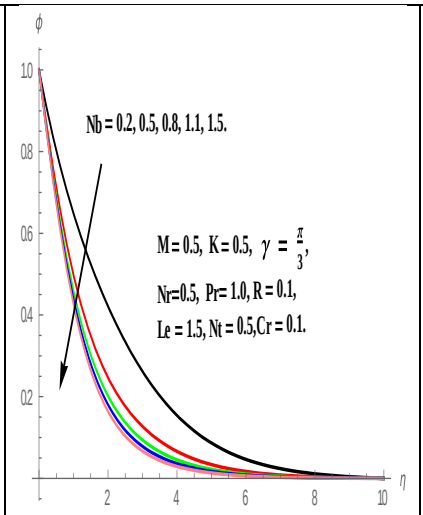

Fig. 12. Effect of Nb on ϕ.

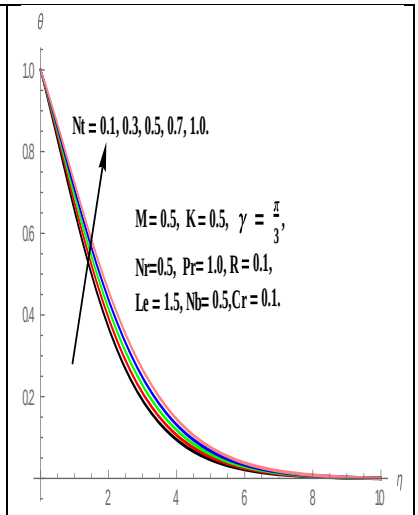

Fig. 13. Effect of Nt on θ.

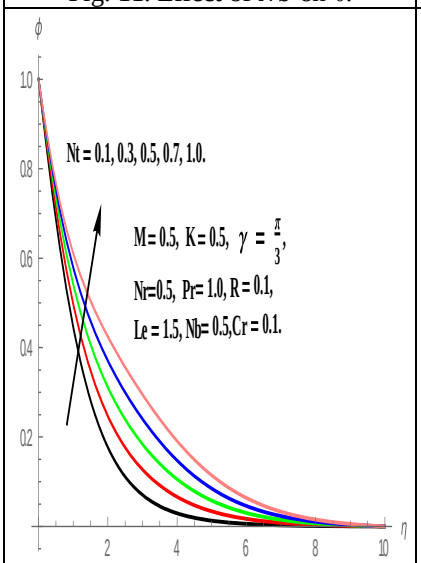

Fig. 14. Effect of Nt on ϕ.

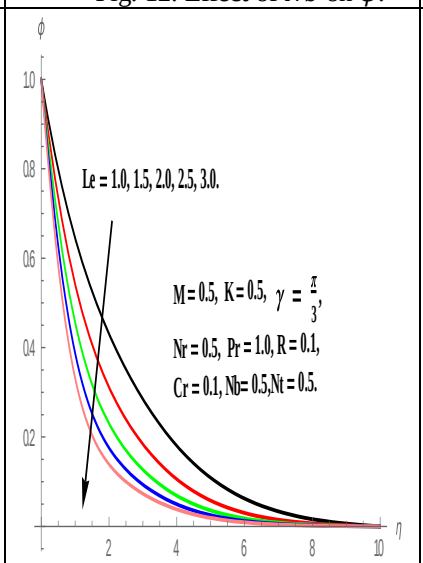

Fig. 15. Effect of Le on ϕ.

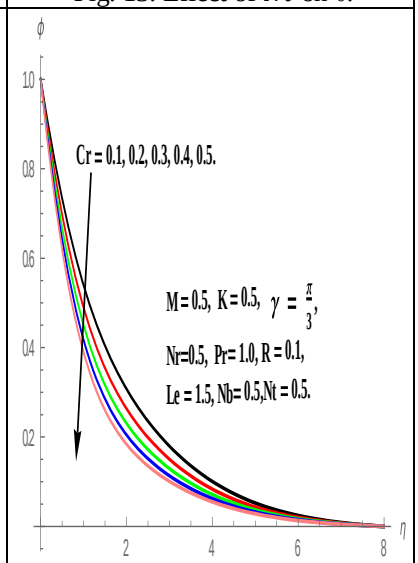

Fig. 16. Effect of Cr on ϕ.